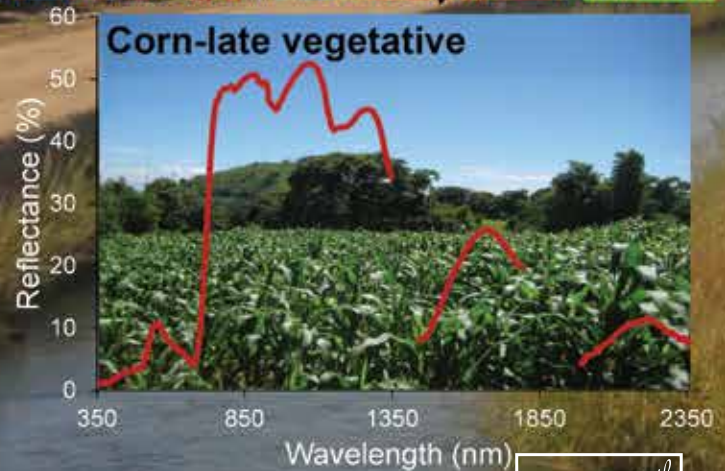
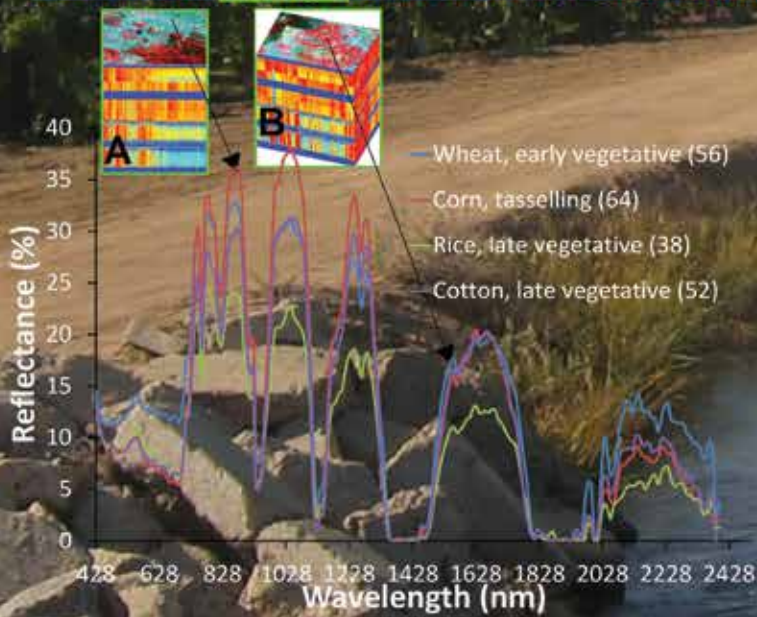
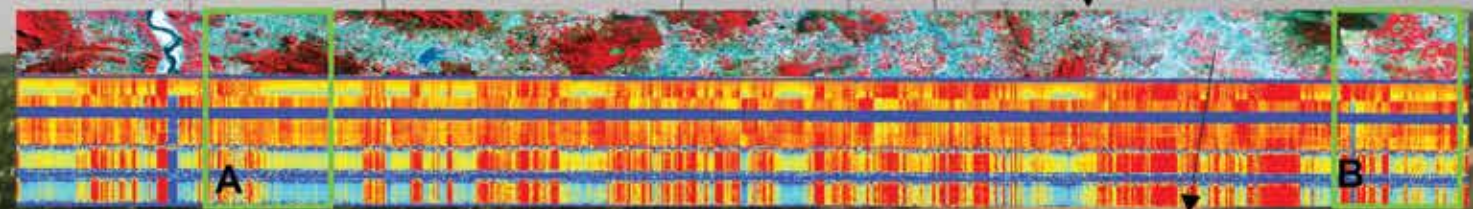
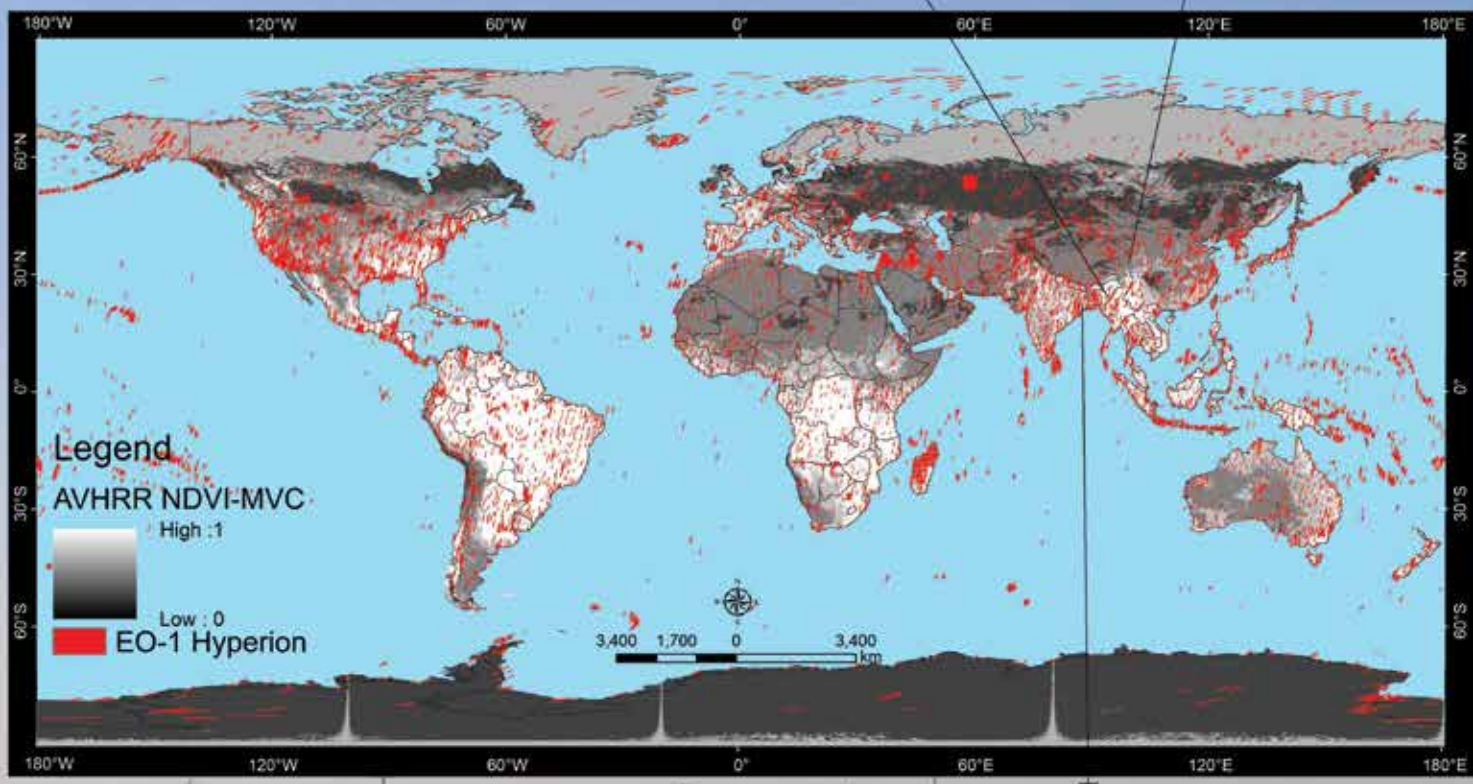
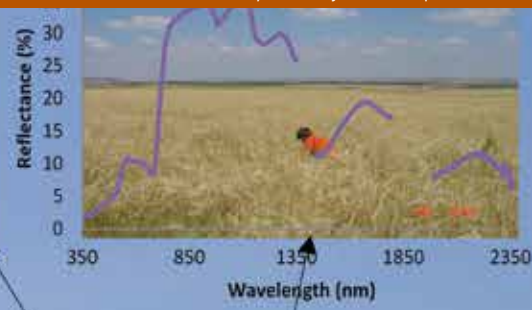
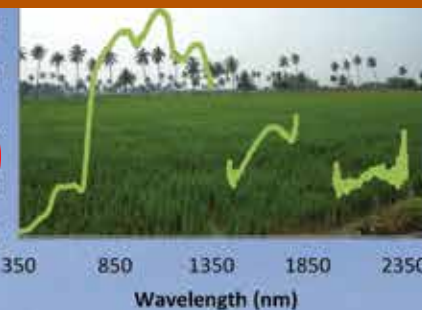


PE&RS

August 2014

Volume 80, Number 8



PHOTOGRAMMETRIC ENGINEERING & REMOTE SENSING

The official journal for imaging and geospatial information science and technology



COLUMNS

Anatoly A. Gitelson, Technion—Israel Institute of Technology	696
Grids and Datums <i>Republic of Chad</i>	712
Mapping Matters	715
Book Review <i>Wavelets and Fractals in Earth System Sciences</i>	716
Behind the Scenes	718

ANNOUNCEMENTS

Pecora 19 & ISPRS Commission I Symposium	693
Call for Papers	724, 744

DEPARTMENTS

Certification	714
Industry News	720
New Members	720
Member Champions	732
Calendar	756
Forthcoming Articles	756
Who's Who in ASPRS	805
Sustaining Members	806
Instructions for Authors	809
Membership Application	812

HIGHLIGHT ARTICLE

697 Hyperspectral Remote Sensing of Vegetation and Agricultural Crops

Prasad S. Thenkabail, Murali Krishna Gumma, Pardhasaradhi Teluguntla, and Irshad A. Mohammed

INTERVIEW

710 John All

SPECIAL ISSUE FOREWORD

721 Research Advances in Hyperspectral Remote Sensing

Prasad S. Thenkabail

PEER-REVIEWED ARTICLES

725 Improved Capability in Stone Pine Forest Mapping and Management in Lebanon Using Hyperspectral CHRIS-Proba Data Relative to Landsat ETM+

Mohamad Awad, Ihab Jomaa, and Fatima Arab

An effective, low cost, and fast method for monitoring the changes in the forest cover, detecting diseases in forests, and mapping different forest species.

733 Combining Hyperspectral and Lidar Data for Vegetation Mapping in the Florida Everglades

Caiyun Zhang

A synergy of hyperspectral and LiDAR systems for automated vegetation mapping in a complex wetland Florida Everglades.

745 Hyperspectral Optical, Thermal, and Microwave L-Band Observations For Soil Moisture Retrieval at Very High Spatial Resolution

Nilda Sánchez, Maria Piles, José Martínez-Fernández, Mercè Vall-llossera, Luca Pipia, Adriano Camps, Albert Aguasca, Fernando Pérez-Aragüés, and Carlos M. Herrero-Jiménez

The potential of merging optical and thermal hyperspectral airborne data with microwave observations for estimating surface soil moisture at very high spatial resolution.

757 Biomass Modeling of Four Leading World Crops Using Hyperspectral Narrowbands in Support of HypsIRI Mission

Michael Marshall and Prasad Thenkabail

Ground-based spectroradiometric and aboveground fresh biomass data for four major world crops studied in the Central Valley of California to identify hyperspectral narrowbands sensitive to biomass using empirically-based modeling techniques.

773 Hyperspectral Data Dimensionality Reduction and the Impact of Multi-seasonal Hyperion EO-1 Imagery on Classification Accuracies of Tropical Forest Species

Manjit Saini, Binal Christian, Nikita Joshi, Dhaval Vyas, Prashanth Marpu, and Krishnaya Nadiminti

EO-1 Hyperion data was used to classify three distinct forest species during 3 seasons (monsoon, winter, summer) and the best classification accuracies were achieved using kernel principal component analysis through maximum likelihood classifier (kPCA-ML) for the monsoon season with overall accuracies of 83 to 100 percent for single species, 74 to 81 percent for two species, and 72 percent for three species respectively.

785 Automated Hyperspectral Vegetation Index Retrieval from Multiple Correlation Matrices with HyperCor

Helge Aasen, Martin Leon Gnyp, Yuxin Miao, and Georg Bareth

Introducing the software HyperCor for automated preprocessing and calculation of correlation matrices from hyperspectral field spectrometry and the multi-correlation matrix strategy for the retrieval of hyperspectral vegetation indices to estimate rice biomass in the tillering, stem elongation, heading, and across all growth stages.

797 Automated Class Labeling Of Classified Landsat Tm Imagery Using a Hyperion-Generated Hyperspectral Library

Iliia Parshakov, Craig Coburn, and Karl Staenz

A new method for the automatic labeling of classified imagery using Z-Score distance is for class label assignment of Landsat-5 TM imagery using Hyperion hyperspectral data.



"Hyperspectral Hyperion Images and Spectral Libraries of Agricultural Crops" is the theme of this month's special issue. Global Image on the cover page shows the location of ~ 64,000 Hyperion sensor (onboard Earth Observing-1 or EO-1; <http://eo1.usgs.gov/> satellite) acquired

images during years 2000-2013. Each image is 7.5 km by 180 km, 242 bands, and 10 nm narrow bandwidth acquiring data in 400-2500 nm spectral range. Images are freely available at: <http://earthexplorer.usgs.gov/> Cover page also shows a sample Hyperion image data cubes for an area within the Krishna river basin, India. Typical crop spectra derived from Hyperion images for some of the leading world crops, at certain phenological growth stages, are depicted in bottom left. Hyperspectral signatures of crops shown with photos in the background are gathered using a hand-held spectroradiometer. For details read the Highlight article in this issue.

Cover page credits: Dr. Prasad S. Thenkabail, U.S. Geological Survey (USGS), Dr. Murali Krishna Gumma, International Center for Research in the Semi-arid Tropics (ICRISAT), Dr. Pardhasaradhi Teluguntla, U.S. Geological Survey (USGS) and Bay Area Environmental Research Institute (BAERI), and Mr. Irshad A. Mohammed, ICRISAT. Contact: pthenkabail@usgs.gov or thenkabail@gmail.com.

HYPERSPECTRAL REMOTE SENSING OF VEGETATION AND AGRICULTURAL CROPS

Prasad S. Thenkabail,
Murali Krishna Gumma,
Pardhasaradhi Teluguntla, and
Irshad A. Mohammed

INTRODUCTION

There are now over 40 years of research in hyperspectral remote sensing (or imaging spectroscopy) of vegetation and agricultural crops (Thenkabail *et al.*, 2011a). Even though much of the early research in hyperspectral remote sensing was overwhelmingly focused on minerals, now there is substantial literature in characterization, monitoring, modeling, and mapping of vegetation and agricultural crops using ground-based, platform-mounted, airborne, Unmanned Aerial Vehicle (UAV) mounted, and spaceborne hyperspectral remote sensing (Swatantran *et al.*, 2011; Atzberger, 2013; Middleton *et al.*, 2013; Schlemmer *et al.*, 2013; Thenkabail *et al.*, 2013; Udelhoven *et al.*, 2013; Zhang *et al.*, 2013). The state-of-the-art in hyperspectral remote sensing of vegetation and agriculture shows significant enhancement over conventional remote sensing, leading to improved and targeted modeling and mapping of specific agricultural characteristics such as: (a) biophysical and biochemical quantities (Galvão, 2011; Clark and Roberts, 2012), (b) crop type\species (Thenkabail *et al.*, 2013), (c) management and stress factors such as nitrogen deficiency, moisture deficiency, or drought conditions (Delalieux *et al.*, 2009; Gitelson, 2013; Slonecker *et al.*, 2013), and (d) water use and water productivities (Thenkabail *et al.*, 2013). At the same time, overcoming Hughes' phenomenon or curse of dimensionality of data and data redundancy (Plaza *et al.*, 2009) is of great importance to make rapid advances in a much wider utilization of hyperspectral data. This is because, for a specific application, a large number of hyperspectral bands are redundant (Thenkabail *et al.*, 2013). Selecting the relevant bands will require the use of data mining techniques (Burger and Gowen, 2011) to focus on utilizing the optimal or best ones to maximize the efficiency of data use and reduce unnecessary computing.



“Hyperspectral Remote Sensing (or Imaging Spectroscopy) is the future of remote sensing, providing continuous data along the electromagnetic spectrum (spectral signatures of objects) rather than few data points averaged over broad wavelengths”

EVOLUTION OF HYPERSPECTRAL SENSORS

Detailed discussions on hyperspectral sensors on various platforms can be found in a number of publications (Ortenberg, 2011; Qi, 2011; Staenz and Held, 2012; Verrelst *et al.*, 2012; Cook *et al.*, 2013; Middleton *et al.*, 2013). An overwhelming proportion of hyperspectral data of vegetation and agricultural crops hitherto has been based on hand-held spectrometers such as the Analytical Spectral Devices (ASD, 2013) suite of instruments as a result of their easy use, absence of hindrance from cloud cover, and as a result of high cost of airborne systems and very few existing spaceborne systems (e.g., Thenkabail *et al.*, 2000;

Table 1. Characteristics of space-borne hyperspectral sensors (either in orbit or planned for launch) compared with ASD spectroradiometer^{a,b}

Sensor	Spatial (meters)	Spectral (#)	Swath (km)	band range (µm)	band widths (µm)	Irradiance (W m ⁻² sr ⁻¹ mm ⁻¹)	Data Points (# per hectares)	Launch (date)
1. Hyperion, EO-1 (USA)	30	220 (196 ^b)	7.5	196 effective Calibrated bands VNIR (band 8 to 57) 427.55 to 925.85 nm; SWIR (band 79 to 224) 932.72 to 2395.53 nm	10 nm wide (approx.) for all 196 bands	See data in Neckel and Labs (1984). Plot it and obtain values for Hyperion bands	11.1	2000-present
2. CHRIS, PROBA (ESA)	25	19	17.5	200-1050	1.25-11	same as above	16	2001-present
3. HypsIRI VSWIR (USA)	60	210	145	210 bands in 380 - 2500 nm	10 nm wide (approx.) for all 210 bands	See data in Neckel and Labs (1984). Plot it	2.77	2020+
4. HypsIRI TIR (USA)	60	8	145	7 bands in 7500-12000 nm and 1 band in 3000-5000 nm (3980 nm center)	7 bands in 7500-12000 nm	See data in Neckel and Labs (1984). Plot it	2.77	2020+
5. EnMAP (Germany)	30	92	30	420-1030	5 - 10	same as above	11.1	2015+
6. PRISMA (Italy)	30	108	30	950-2450	10 - 20	same as above	11.1	2014+
7. ASD spectroradiometer	1134 cm ² @ 1.2 m Nadir view 18 degree Field of view	2100 effective 1 nm width between 400-2500 nm	N/A	2100 effective bands	1 nm wide (approx.) in 400-2500nm	See data in Neckel and Labs (1984). Plot it and obtain values for Hyperion bands	88183	last 30+ years

Note:

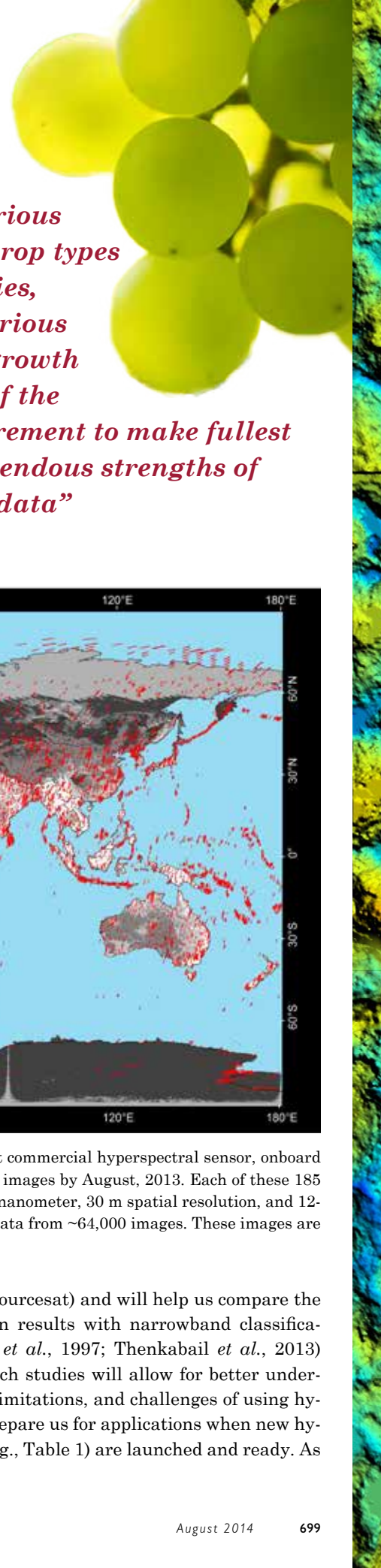
a = information for the table from *Hyperspectral Remote Sensing of Vegetation* book edited by Thenkabail et al., 2011.

b = Of the 242 bands, 196 are unique and calibrated. These are: (A) Band 8 (427.55 nm) to band 57 (925.85 nm) that are acquired by visible and near-infrared (VNIR) sensor; and (B) Band 79 (932.72 nm) to band 224 (2395.53 nm) that are acquired by short wave infrared (SWIR) sensor.

Poças *et al.*, 2012). These spectrometers, typically, operate from 400 to 2500 nm with a very narrow bandwidth of 1 to 10 nanometers. Further, there is an emerging hyperspectral capability that has shown potential for vegetation information in the Thermal Infrared spectrum or TIR (e.g., Thermo-Nicolet Nexus 670 FTIR 250-25000 nm) (Hecker *et al.*, 2013; Hook *et al.*, 2013; Slonecker *et al.*, 2013) and there are also emerging overhead sensors, such as spatially enhanced broadband array spectrograph system (SEBASS) that bring a new set of hyperspectral capabilities to the table.

Over the years, NASA has been extensively using the Airborne Visible/Infrared Imaging Spectrometer (AVIRIS), and, more recently, AVIRIS next generation (AVIRIS NG), and the

MODIS/ASTER Airborne Simulator (MASTER) instruments. The airborne sensors can cover areas repeatedly, but are costly and not easy to routinely schedule acquisition. There are also hyperspectral imaging (HIS) sensors with limited spectrum bandwidths, such as the CAP/Archer, that are providing low-end hyperspectral data at reasonable costs. More recently, there have been efforts to fly hyperspectral imagers onboard UAVs, which offer a new platform to gather data in real time repeatedly without limitation of cloud cover issues. However, the technology is still under development with a wide array of issues ranging from geometric registration, calibration over large areas, limitation of large area coverage to security concerns of operating UAVs.



Given the above facts, spaceborne hyperspectral platforms (e.g., Table 1; also see Ortenberg, 2011; Qi, 2011) offer powerful option for repeated, consistent global coverage. For example, already there are now ~64,000 Hyperion images (Figure 1) acquired by the Earth Observing-1 (EO-1; Middleton *et al.*, 2013) satellite from 2000 to 2013. These images, each of 7.5 km by 180 km in 242 bands over 400 to 2500 nm, offer a great opportunity to study terrestrial land features including vegetation and agricultural crops around the world with much greater detail and higher accuracies than any multispectral sensor (Thenkabail *et al.*, 2011b). For example, it is feasible to establish a significant spectral library of agricultural crops (Figure 2 derived from Hyperion images) around the world using Hyperion images with adequate prior knowledge about what was grown where and when (which in turn can be gathered from field data from national databases for many places in the world). However, the poor signal to noise ratio of Hyperion as well as atmospheric effects influencing the signatures

“Development of precise spectral libraries of various vegetation or crop types and their species, gathered at various phenological growth stages, is one of the primary requirement to make fullest use of the tremendous strengths of hyperspectral data”

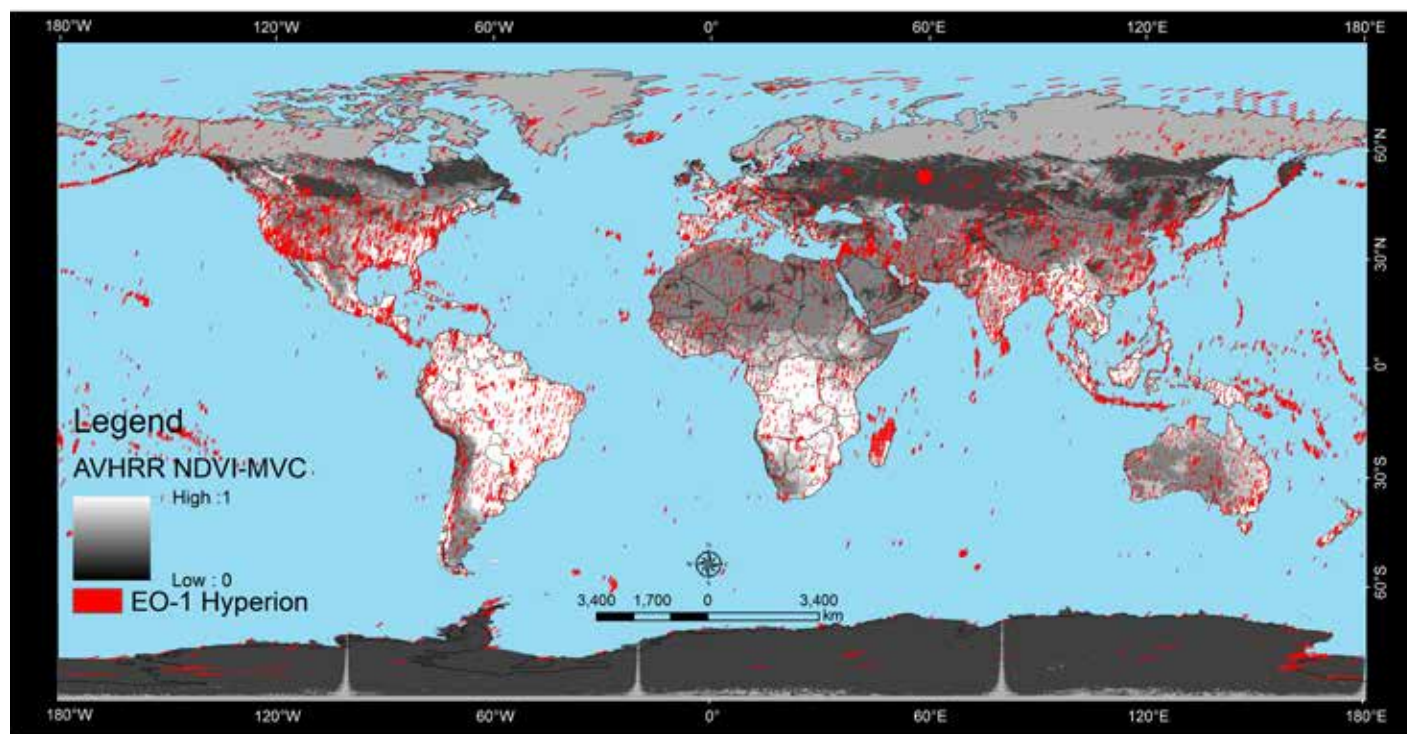


Figure 1. Hyperion hyperspectral image coverage of the World from 2001-2013. Hyperion, the first commercial hyperspectral sensor, onboard Earth Observing-1 (EO-1) was launched on November 21, 2000 and has acquired a total of ~64,000 images by August, 2013. Each of these 185 km x 7.5 km image tiles has a total of 242 bands, with each being 10 nm widespread over 400-2500 nanometer, 30 m spatial resolution, and 12-bits radiometric resolution. With each image having 5.25 gigabyte of data, there is 336 terabyte of data from ~64,000 images. These images are freely downloadable from USGS EarthExplorer (<http://earthexplorer.usgs.gov/>).

need to be kept in mind. Similarly, much of the forest vegetation (e.g., species composition) or other natural vegetation in specific locations may remain the same over years. Hence, one could use the collection of ~64,000 Hyperion images (Figure 1) to establish spectral libraries of specific forest or other vegetation species or categories. Also, hyperspectral images such as Hyperion will allow us to simulate other broadband data (e.g.,

Landsat, IKONOS, Resourcesat) and will help us compare the broadband classification results with narrowband classification results (Bruzzone *et al.*, 1997; Thenkabail *et al.*, 2013) over the same area. Such studies will allow for better understanding of strengths, limitations, and challenges of using hyperspectral data and prepare us for applications when new hyperspectral missions (e.g., Table 1) are launched and ready. As

can be seen in various spectral signatures (Figure 2) there are distinct differences between various vegetation categories or species at specific portions of the spectrum. For example, cotton, rice, and wheat crops are best discriminated using SWIR bands (e.g., 1520 nm, 1820 nm) than anywhere in visible and NIR bands. Similarly, others have shown (Thenkabail *et al.*, 2004a; Pu and Bell, 2013; Thenkabail *et al.*, 2013) primary forest was most distinctive from secondary forest at wavebands centered around 1045 nm, 1640 nm, and 2130 nm. This tells us that hyperspectral data offers many windows of opportunity to spectrally distinguish complex vegetation. However, it requires rigorous quantitative analysis after addressing data normalization and harmonization issues including radiometric and atmospheric corrections (Thenkabail *et al.*, 2004a; Pu and Bell, 2013; Thenkabail *et al.*, 2013), and numerous data mining approaches (Bajwa and Kulkarni, 2011).

and Thenkabail, 2014). Data mining methods lead to: (a) reduction in data dimensionality (Bajwa and Kulkarni, 2011), (b) reduction in data redundancy (Burger and Gowen, 2011), and (c) extraction of unique information. However, these data mining approaches often reduce data without identifying which wavebands are redundant and which have unique information content. This requires us to identify redundant bands and separate them from valuable bands, a concept first proposed by Thenkabail *et al.* (e.g., 2000) and applied by numerous researchers later on. Often, bands that adjoin one another (e.g., a 10 nm wide narrow bands centered at 680 nm and a 10 nm wide narrowband centered at 690 nm) are nearly perfectly correlated (R-square >0.99) (Thenkabail *et al.*, 2013). Since such bands provide similar information, it is best to select one unique band, i.e., the band that provides maximum information. A series of research papers by (Thenkabail *et al.*,

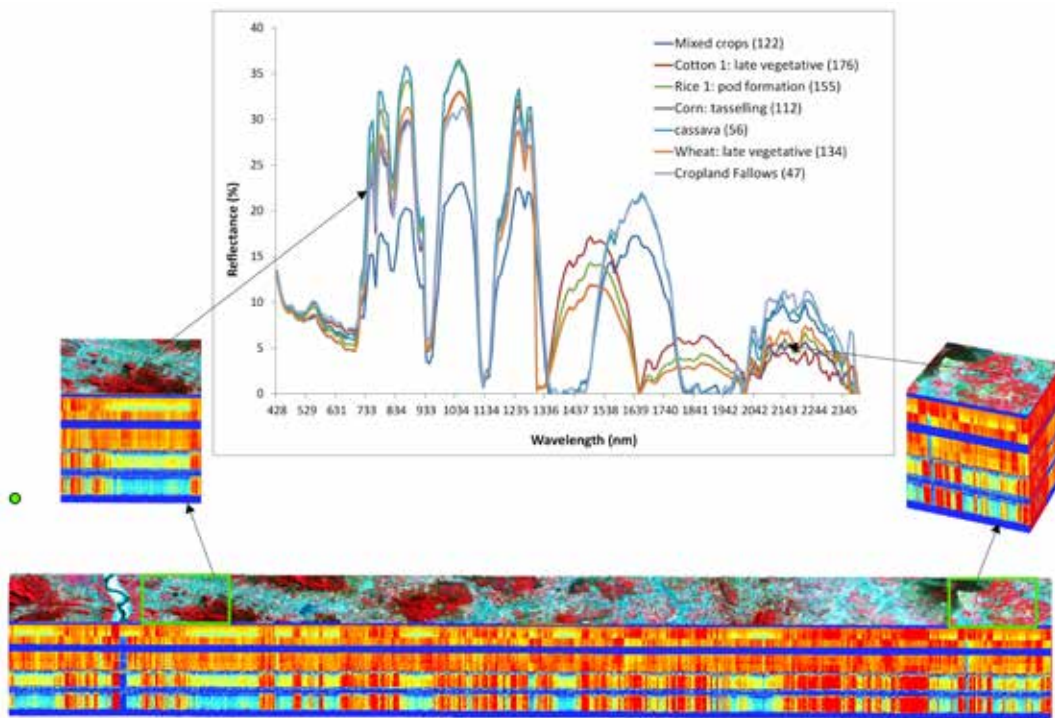


Figure 2. Hyperspectral data cube derived from Hyperion images for an agricultural area.

“Typically, ~3 to 8 HNBs help attain best possible R-square values in modeling agricultural crop biophysical and biochemical variables, beyond which the relationship becomes asymptotic”

DATA REDUNDANCY AND OPTIMAL (OR BEST) HYPERSPECTRAL NARROWBANDS (HNBs)

The need to address large data volumes that separates real data from noise in hyperspectral imagery cannot be over-emphasized. Data volumes are reduced through data mining methods such as feature selection (e.g., principal component analysis, derivative analysis, wavelets, the lambda by lambda correlation plots; (Thenkabail *et al.*, 2000), and partial least squares and vegetation indices (Mundt *et al.*, 2006; Bajwa and Kulkarni, 2011; Swatantran *et al.*, 2011; Banskota *et al.*, 2013; Thenkabail *et al.*, 2013; Thorp *et al.*, 2013; Marshall

2000; Thenkabail, 2002; Thenkabail *et al.*, 2004a; Thenkabail *et al.*, 2004b; Thenkabail *et al.*, 2013) conducted rigorous accuracy assessments (Congalton and Green, 1999; Congalton and Green, 2008) and established that ~15 to 20 narrowbands (e.g., Figure 3) out of 242 Hyperion HNBs provide optimal information in classifying crops and vegetation (leaving ~220 HNBs redundant). For example, seven vegetation categories (Figure 3), when classified using 157 calibrated, non-atmospheric window portions of Hyperion bands, achieved an accuracy of 92% for 15 best bands (Figure 3). Research by Thenkabail *et al.* (2013, 2011, 2004, 2002) identified ~15 to 20 HNBs as optimal (e.g., Figure 3), but meta-analysis based on a wide array of research papers consider up to 28 HNBs (Table 2, Figure 4a) as non-redundant. Relative to HNBs,

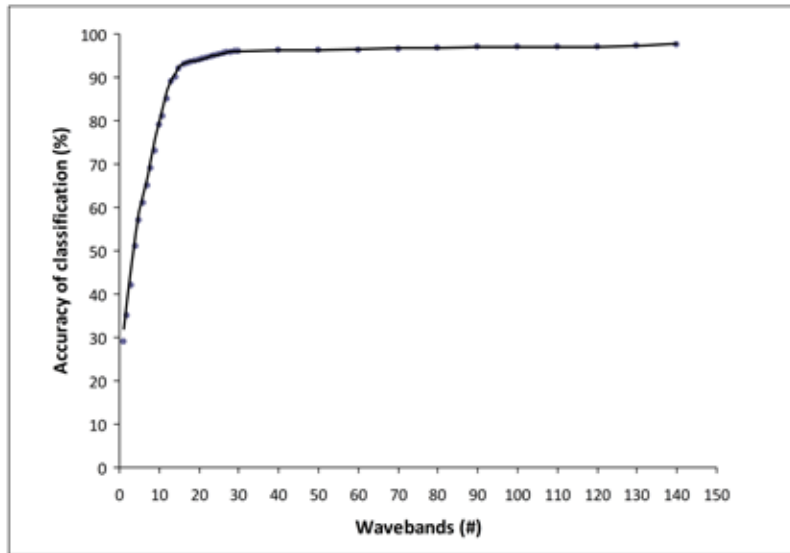


Figure 3. Figure depicting information content relative to the number of Hyperion bands for classifying 7 vegetation classes in Central Africa. The 7 vegetation classes are: slash and burn agriculture, agricultural fallows (1-3 years), agricultural fallows (>3 years), wetlands, young secondary forest, mature secondary forest, and primary forest. About 15 hyperspectral Hyperion bands achieve 92% accuracy, beyond which the additional bands provide little or no increase in accuracy.



“Eliminating the redundant bands, and establish optimal bands, is an important step in hyperspectral data analysis. Overall, ~15 to 20, but no more than about 28 HNBs provide optimal information in study of vegetation or crop characterization and classification”

Table 2. Optimal (non-redundant) hyperspectral narrow bands to study vegetation and agricultural crops^{1,2,3,4,5,6}

Waveband number (#)	Waveband center (λ)	Waveband width ($\Delta\lambda$)	Importance and physical significance of waveband in vegetation and cropland studies
A. Ultraviolet			
1	375	5	fPAR, leaf water: fraction of photosynthetically active radiation (fPAR), leaf water content
B. Blue bands			
2	405	5	Nitrogen, Senescing: sensitivity to changes in leaf nitrogen. reflectance changes due to pigments is moderate to low. Sensitive to senescing (yellow and yellow green leaves).
3	490	5	Carotenoid, Light use efficiency (LUE), Stress in vegetation: Sensitive to senescing and loss of chlorophyll\browning, ripening, crop yield, and soil background effects
C. Green bands			
4	515	5	Pigments (Carotenoid, Chlorophyll, anthocyanins), Nitrogen, Vigor: positive change in reflectance per unit change in wavelength of this visible spectrum is maximum around this green waveband
5	531	1	Light use efficiency (LUE), Xanophyll cycle, Stress in vegetation, pest and disease: Senescing and loss of chlorophyll\browning, ripening, crop yield, and soil background effects
6	550	5	Chlorophyll: Total chlorophyll; Chlorophyll/carotenoid ratio, vegetation nutritional and fertility level; vegetation discrimination; vegetation classification
7	570	5	Pigments (Anthocyanins, Chlorophyll), Nitrogen: negative change in reflectance per unit change in wavelength is maximum as a result of sensitivity to vegetation vigor, pigment, and N.
D. Red bands			
8	682	5	Biophysical quantities and yield: leaf area index, wet and dry biomass, plant height, grain yield, crop type, crop discrimination
E. Red-edge bands			
9	705	5	Stress and chlorophyll: Nitrogen stress, crop stress, crop growth stage studies
10	720	5	Stress and chlorophyll: Nitrogen stress, crop stress, crop growth stage studies
11	700-740	700-740	Chlorophyll, senescing, stress, drought: first-order derivative index over 700-740 nm has applications in vegetation studies (e.g., blue-shift during stress and red-shift during healthy growth)

F. Near infrared (NIR) bands			
12	855	20	Biophysical quantities and yield: leaf area index, wet and dry biomass, plant height, grain yield, crop type, crop discrimination, total chlorophyll Moisture, biomass, and protein: peak NIR reflectance. Useful for computing crop moisture sensitivity index.
13	910	5	
G. Near infrared (NIR) bands			
14	970	10	Water, Moisture and biomass: Center of moisture sensitive “trough”; water band index, leaf water, biomass
H. Far near infrared (FNIR) bands			
15	1075	5	Biophysical and biochemical quantities: leaf area index, wet and dry biomass, plant height, grain yield, crop type, crop discrimination, total chlorophyll, anthocyanin, carotenoids Water absorption band Water sensitivity: water band index, leaf water, biomass. Reflectance peak in 1050-1300 nm.
16	1180	5	
17	1245	5	
I. Early short-wave infrared (ESWIR) bands			
18	1450	5	Vegetation classification and discrimination: ecotype classification; plant moisture sensitivity. Moisture absorption trough in early short wave infrared (ESWIR) Moisture and biomass: A point of most rapid rise in spectra with unit change in wavelength in SWIR. Sensitive to plant moisture. Heavy metal stress, Moisture sensitivity: Heavy metal stress due to reduction in Chlorophyll. Sensitivity to plant moisture fluctuations in ESWIR. Use as an index with 1548 or 1620 or 1690 nm.. Lignin, biomass, starch, moisture: sensitive to lignin, biomass, starch. Discriminating crops and vegetation.
19	1518	5	
20	1650	5	
21	1725	5	
J. Far short-wave infrared (FSWIR) bands			
22	1950	5	Water absorption band: highest moisture absorption trough in FSWIR. Use as an index with any one of 2025 nm, 2133 nm, and 2213 nm. Affected by noise at times. Litter (plant litter), lignin, cellulose: litter-soil differentiation: moderate to low moisture absorption trough in FSWIR. Use as an index with any one of 2025 nm, 2133 nm, and 2213 nm. Litter (plant litter), lignin, cellulose: typically highest reflectivity in FSWIR for vegetation. Litter-soil differentiation Litter, lignin, cellulose, sugar, starch, protein; Heavy metal stress: typically, second highest reflectivity in FSWIR for vegetation. Heavy metal stress due to reduction in Chlorophyll Moisture and biomass: moisture absorption trough in far short-wave infrared (FSWIR). A point of most rapid change in slope of spectra based on land cover, vegetation type, and vigor. Stress: sensitive to soil background and plant stress Cellulose, protein, nitrogen: sensitive to crop stress, lignin, and starch
23	2025	5	
24	2133	5	
25	2205	5	
26	2260	5	
27	2295	5	
28	2359	5	

Note:

- 1 = most hyperspectral narrowbands (HNBs) that adjoin one another are highly correlated for a given application. Hence from a large number of HNBS, these non-redundant (optimal) bands are selected
- 2 = these optimal HNBS are for studying vegetation and agricultural crops. When we use these wavebands, we can attain highest possible classification accuracies in classifying vegetation categories or crop types
- 3 = wavebands selected here are based on careful evaluation of large number of studies. These studies are widely discussed and referenced in Thenkabail et al. 2011, Thenkabail et al., 2012, Thenkabail et al., 2013, Marshall and Thenkabail, 2014, Thenkabail et al., 2004a, Thenkabail et al., 2004b, Thenkabail et al., 2002, and Thenkabail et al., 2000.
- 4 = for details on physical relevance of these wavebands please refer to Thenkabail et al. 2011, Thenkabail et al., 2012
- 5 = the hyperspectral vegetation indices (HVIs) recommended in Table 2 are derived using these HNBS
- 6 = this Table is derived, modified, and revised based on recent work discussed in Thenkabail et al., 2013, Marshall and Thenkabail, 2014, Thenkabail et al., 2004a, Thenkabail et al., 2004b, Thenkabail et al., 2002, and Thenkabail et al., 2000.

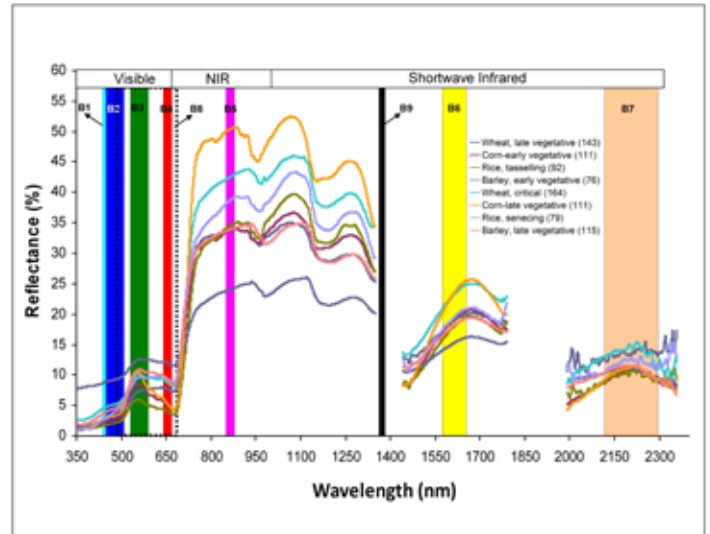
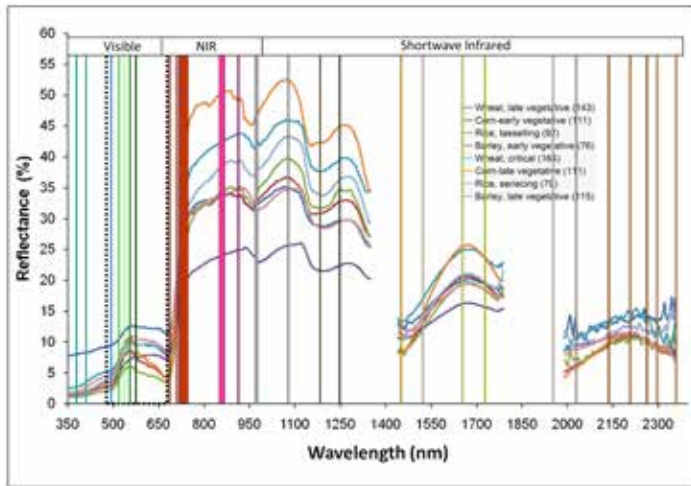


Figure 4. Optimal hyperspectral narrowbands (HNBS; Figure 4a) and Landsat-8 broadbands (BBs; Figure 4b): showing the band centers and widths. These band centers and widths are plotted on spectroradiometer measured hyperspectral signatures for certain key crops. The 28 bands shown in Figure 4a are derived from Table 2. The 9 non-thermal bands of the Landsat-8 are shown in Figure 4b.

broadbands (e.g., 6 non-thermal Landsat), typically, achieve ~30% fewer accuracies (Thenkabail *et al.*, 2004b). Methods of classification of vegetation using HNBS include multivariate or partial least square regressions, discriminant analysis, unsupervised classification, supervised approaches, spectral angle mapper (SAM), artificial neural networks, and support vector machines (SVM) (Zhang *et al.*, 2000; Thenkabail *et al.*, 2011b).

“Hughes’ Phenomenon: With the increased number of hyperspectral narrowbands the number of samples (i.e., training pixels) required to maintain minimum statistical confidence and functionality in hyperspectral data for classification purposes grows exponentially, making it very difficult to address this issue adequately. This problem is known as Hughes’ Phenomenon and can be addressed by overcoming data redundancy and/or through obtaining large number of training pixels for each class”.

HUGHES’ PHENOMENON

Hyperspectral data can have 100s or even 1000s of bands. However, with increased number of hyperspectral narrowbands the number of samples (i.e., training pixels) required to maintain minimum statistical confidence and functionality in hyperspectral data for classification purposes grows exponentially, making it very difficult to address this issue adequately. For example, if we were to classify 10 land cover classes using 100s or 1000s of HNBS, we will require very large training samples for each class in order to establish statistical integrity of classification, whereas broadband data like Landsat can be classified with significantly fewer training samples for every class. Also, greater dimension of hyperspectral data allows greater number of classes to be achieved. Naturally, it is of great advantage to have a large number of HNBS to classify complex land cover classes. However, its statistical integrity can only be maintained if each class has enough training samples to train the classifier and equally large number of training samples for each class to establish the class accuracy. So, what is a blessing can also turn to a curse. This phenomenon is known as *Hughes’ phenomenon* or *curse of dimensionality* of data (Thenkabail *et al.*, 2011b; Thenkabail *et al.*, 2013). Nevertheless, it must be stated that modern access to multitude ways of instantaneous gathering of image data (e.g., potential from hundreds and even thousands of micro satellites such as Planet Labs gathering images over Planet), evolution of super-computing on desktop and mobile platforms, and smart algorithms will help overcome this “curse”.

HYPERSPECTRAL NARROWBANDS IN THE STUDY OF VEGETATION AND AGRICULTURAL CROPS

Over the years, extensive research has been conducted in identifying optimal (best) HNBs for study of vegetation and agricultural crops (Thenkabail *et al.*, 2000; Thenkabail, 2002; Thenkabail *et al.*, 2004a; Thenkabail *et al.*, 2004b; Blackburn, 2007; Thenkabail *et al.*, 2011b; Miphokasap *et al.*, 2012; Gitelson, 2013; Mariotto *et al.*, 2013; Thenkabail *et al.*, 2013; Marshall and Thenkabail, 2014). A review of these and meta-analysis leads to 28 HNBs (Table 2, Figure 4a) that are non-redundant and optimal in studying a wide range of agricultural crops and vegetation. An overwhelming proportion of the 28 HNBs were in short-wave infrared: 7 in far SWIR (FSWIR), and 4 in early SWIR (ESWIR). This was followed by 4 in green, 3 each in far near infrared (FNIR), near infrared (NIR), and red-edge, 1 in red, and 1 in ultraviolet (Table 2, Figure 4a). The advantage of using optimal spectral analysis (OSA) involving optimal HNBs (Figure 4a, Table 2), as opposed to continuous spectra (i.e., every HNB in 400 to 2500 nm) or whole spectra analysis (WSA), are several. These include:

1. Avoiding a large number of redundant data (~88%) and focusing on utilizing non-redundant bands (~12%), which in turn helps in overcoming Hughes' phenomenon;
2. Constituting specific hyper spectral vegetation's indices (HVI) from HNBs;
3. Obtaining the same or nearly the same classification accuracies using optimal 28 HNBs as opposed to a full range of bands (e.g., 242 bands of Hyperion), because accuracies asymptote after a certain number of wavebands (e.g., ~15 to 20 HNBs attain >90% accuracy in classifying 7 vegetation classes as shown in Figure 3); and
4. Increasing the computation speed and optimizing the resources in computing and analyzing;

Nevertheless, there is considerable debate for using whole spectra analysis (e.g., continuous and entire spectra over 700-740 nm) using such methods as partial least squares regression, wavelet analysis, continuum removal, and spectral angle mapper (Nielsen, 2001; Delalieux *et al.*, 2009; Thenkabail *et al.*, 2011b; Mirzaie *et al.*, 2014). The use of WSA is justified when:

1. Spectral signatures of objects need to be matched with spectral signatures from existing spectral library;
2. Integrated spectra over a continuum (e.g., first-order derivative greenness vegetation index over 600 to 760 nm, 700 to 740 nm, or integrated over other HNBs) need to be taken advantage of; and
3. Computing power and other resources are not a limitation.

It must be noted that the 28 HNBs (Table 2, Figure 4a) discussed here are limited to the 400 to 2500 nm spectral domain. There is substantial potential to use thermal

hyperspectral wavebands (Schlerf *et al.*, 2012) in addition to these HNBs. Therefore, there should be considerable effect for further advances in developing optimal HNBs in the study of vegetation and agricultural crops if we include thermal hyperspectral bands. Moreover, recent efforts involve combining LiDAR, Hyperspectral, and Thermal (G-LiHT) imagery (Cook *et al.*, 2013), which will further advance our understanding in classifying, monitoring, modeling, and mapping vegetation and agricultural crops (Ribeiro da Luz and Crowley, 2010).

HYPERSPECTRAL VEGETATION INDICES IN THE STUDY OF VEGETATION AND AGRICULTURAL CROPS

Hyperspectral vegetation indices (HVIs) (Haboudane *et al.*, 2004; Bian *et al.*, 2010; Galvão, 2011; Roberts, 2011; Thenkabail *et al.*, 2011b; Gitelson, 2013; Thenkabail *et al.*, 2013) allow us to target studies on very specific characteristics of vegetation and agricultural crops such as biomass, leaf area index (LAI), pigments (e.g., chlorophyll, carotenoid, anthocyanin), stress (e.g., due to drought, disease), management properties (e.g., nitrogen, tillage), and other biochemical properties (e.g., lignin, cellulose, plant residue) (Haboudane *et al.*, 2004; Blackburn, 2007; Thenkabail *et al.*, 2011b). There is a potential to have an index for each of these characteristics (Table 3). The biggest limitation of broad band indices derived from sensors such as Landsat is, more or less, that one index such as NDVI is used for studying all vegetation or crop characteristics. In contrast, HVIs have following specific advantages (Table 3):

1. Establish unique indices to study specific vegetation or crop variable (e.g., hyperspectral water moisture indices or HWMI) to study plant water or moisture; hyperspectral biomass and structural indices or HBSI) to study biomass; hyperspectral biochemical indices or HBCI) to study plant pigments and so on; see Table 3).
2. Provide significant improvement by explaining ~10% to 30% greater variability over broadband indices in modeling and mapping vegetation biophysical and biochemical properties (Haboudane *et al.*, 2004; Thenkabail *et al.*, 2011b; Bolton and Friedl, 2013; Mariotto *et al.*, 2013; Thenkabail *et al.*, 2013); and
3. Create better opportunity to develop multi-band indices. Typically, 2 to 8 bands provide best information in terms of R-square values, beyond which addition of bands does not increase the R-square and the relationship becomes asymptotic (Thenkabail *et al.*, 2004a; Thenkabail *et al.*, 2004b; Mariotto *et al.*, 2013; Marshall and Thenkabail, 2014).

Table 3. Hyperspectral vegetation indices or HVIs 1,2,3,4,5

Band number (#)	Hyperspectral narrowband (λ_1)	Bandwidth ($\Delta\lambda_1$)	Hyperspectral narrowband (λ_2)	Bandwidth ($\Delta\lambda_2$)	Hyperspectral vegetation index (HVI)	Best index under each category
I. Hyperspectral biomass and structural indices (HBSIs) [to best study biomass, LAI, plant height, and grain yield]						
HBSI1	855	20	682	5	(855-682)/(855+682)	HBSI: Hyperspectral biomass and structural index
HBSI2	910	20	682	5	(910-682)/(910+682)	
HBSI3	550	5	682	5	(550-682)/(550+682)	
HBSI4	1075	5	682	5	(1075-682)/(1075+682)	
HBSI5	1245	5	682	5	(1245-682)/(1245+682)	
HBSI6	1650	5	682	5	(1650-682)/(1650+682)	
HBSI7	2205	5	682	5	(2205-682)/(2205+682)	
II. Hyperspectral biochemical indices (HBCIs) [pigments like carotenoids, anthocyanins as well as Nitrogen, chlorophyll]						
HBCI8	550	5	515	5	(550-515)/(550+515)	HBCI: Hyperspectral biochemical index
HBCI9	550	5	490	5	(550-490)/(550+490)	
HBCI10	720	5	550	5	(720-550)/(720+550)	
HBCI11	550	5	375	5	(550-375)/(550+375)	
HBCI12	855	20	550	5	(855-550)/(855+550)	
HBCI13	550	5	682	5	(550-682)/(550+682)	
III. Hyperspectral Red-edge indices (HREIs) [to best study plant stress, drought]						
HREI14	700-740	40	first-order derivative integrated over red-edge (700-740 nm)			HREI: Hyperspectral red-edge index
HREI15	855	5	720	5	(855-720)/(855+720)	
HREI16	910	5	705	5	(910-705)/(910+705)	
IV. Hyperspectral water and moisture indices (HWMI) [to best study plant water and moisture]						
HWMI17	855	20	970	10	(855-970)/(855+970)	HWMI: Hyperspectral water and moisture index
HWMI18	1075	5	970	10	(1075-970)/(1075+970)	
HWMI19	1075	5	1180	5	(1075-1180)/(1075+1180)	
HWMI20	1245	5	1180	5	(1245-1180)/(1245+1180)	
HWMI21	1650	5	1450	5	(1650-1450)/(1650+1450)	
HWMI22	2205	5	1450	5	(2205-1450)/(2205+1450)	
HWMI23	2205	5	1950	5	(2205-1950)/(2205+1950)	
V. Hyperspectral Light-use efficiency Index (HLEI) [to best study light use efficiency or LUE]						
HLUE24	570	5	531	1	(570-531)/(570+531)	HLEI: Hyperspectral light-use efficiency index
VI. Hyperspectral legnin cellulose index (HLCI) [to best study plant legnin, cellulose, and plant residue]						
HLCI25	2205	5	2025	1	(2205-2025)/(2205+2025)	HLCI: Hyperspectral legnin cellulose index

Note:

- 1 = adopted with modifications from comprehensive research reported in Thenkabail et al., 2012, Thenkabail et al., 2011;
- 2 = physical relevance of these two band hyperspectral indices are presented and discussed in Table IV in Thenkabail et al. 2012; and various chapters in the book by Thenkabail et al. 2011
- 3 = the first index under each of the six categories performs the best; but further research needs to confirm this
- 4 = for extensive research on hyperspectral wavebands and vegetation indices refer to papers by Thenkabail et al., 2002, 2004, 2011, 2013
- 5 = Under each of the 6 categories (I to VI), you may select the best index (mentioned first in the category and highlighted)

Table 4. Best hyperspectral narrowband (HNB) combinations.

Best 4 bands	550, 682, 855, 970
Best 6 bands	550, 682, 855, 970, 1075, 1450
Best 8 bands	550, 682, 855, 970, 1075, 1180, 1450, 2205
Best 10 bands	550, 682, 720, 855, 970, 1075, 1180, 1245, 1450, 2205
Best 12 bands	550, 682, 720, 855, 910, 970, 1075, 1180, 1245, 1450, 1650, 2205
Best 16 bands	490, 515, 550, 570, 682, 720, 855, 910, 970, 1075, 1180, 1245, 1450, 1650, 1950, 2205
Best 20 bands	490, 515, 531, 550, 570, 682, 720, 855, 910, 970, 1075, 1180, 1245, 1450, 1650, 1725, 1950, 2205, 2260, 2359

HYPERSPECTRAL NARROWBAND COMBINATIONS

Various 4, 6, 8, 10, 12, 16, and 20 best HNB combinations (Table 4) can be required to compare with various corresponding broadband data available to us such as the 9 non-thermal bands of Landsat-8 OLI, 4 band IKONOS, and 4 band IRS. Meta-analysis of literature (e.g., Thenkabail *et al.*, 2011b; Thenkabail *et al.*, 2013) indicates various HNB best-band combinations (Table 4). These HNB combinations work the best in classifying or modeling vegetation or agricultural crops when they come from various portions of the spectrum (e.g., visible, near infrared, shortwave infrared). The number of HNB bands to use and their combinations will depend on the complexity of vegetation or crop types involved. For example, in order to classify 2 crop types over a small area with high degree of accuracy, only the best 4 bands may suffice. But when multiple crops are involved, 16 or 20 bands or even all

“It is obvious that there is a need for Whole Spectral Analysis (WSA) as well as Optimal Spectral Analysis (OSA)”



28 bands (Table 2, Figure 4a) maybe required. In modeling biophysical or biochemical quantities of vegetation or crops, one can compose HVIs (Table 3) based on two band combinations (Table 3) or multiple bands (Table 2, Table 4). It is possible to establish multiple HNB band based indices in modeling crop or vegetation biophysical or biochemical quantities. However, past researches (Thenkabail *et al.*, 2000; Thenkabail *et al.*, 2002; Thenkabail *et al.*, 2004a; Thenkabail *et al.*, 2004b; Bian *et al.*, 2010; Clark and Roberts, 2012; Mariotto *et al.*, 2013; Marshall and Thenkabail, 2014) have shown that R-square values are maximum anywhere between the use of ~3 to 8 bands (Thenkabail *et al.*, 2004b; Mariotto *et al.*, 2013; Marshall and Thenkabail, 2014), beyond which the relationship between the number of HNBs and R-square is asymptotic.

CONCLUSIONS

A summary of the strengths, limitations, and challenges involved in hyperspectral remote sensing (or imaging spectroscopy) of vegetation and agricultural crops is provided in this paper.

The paper identifies optimal HNB- centers and widths (Figure 4b, Table 2) and HVIs (Table 4) that are best for classifying, separating, monitoring, modeling, and mapping vegetation and agricultural crops. Overall, ~15 to 20, but no more than about 28 HNBs (Table 2) provide optimal information in vegetation or crop classification. Typically, HNBs achieve about ~30% higher accuracies compared to 6 non-thermal broadbands in classifying 5 to 12 vegetation or crop categories. Beyond these optimal HNBs, the accuracies asymptote with an increase in the number of HNBs.

There are specific HVIs (Table 3) that best characterize and model vegetation and crop biophysical and biochemical properties. These HVIs are grouped into 6 distinct categories:

1. Hyperspectral biomass and structural indices (HBSIs),
2. Hyperspectral biochemical indices (HBCIs),
3. Hyperspectral red-edge indices (HREIs),
4. Hyperspectral water and moisture indices (HWBIs),
5. Hyperspectral light-use efficiency index (HLUEI), and
6. Hyperspectral lignin-cellulose index (HLCI).

It must be noted, that the use of the first index from each of the six categories is, typically, the best index for the category

(i.e., first index in each of the 6 categories in Table 3). Further, HVIs involving multiple HNBs (Table 4) have great promise and need further research. Typically, in biophysical and biochemical modeling ~3 to 8 bands help attain high R-square values before the relationship becomes asymptotic.

It is now reasonable to state, based on meta analysis, that ~12% of the HNBs in EO-1 Hyperion (i.e., for example, ~30 HNBs out of a total of 242 HNBs each of 10 nm wide from 400-2500 nm) are non-redundant for a given application such as in study of vegetation or agricultural crops. This would mean that about 88% of Hyperion bands (e.g., ~212 HNBs out of a total of 242 HNBs) are redundant. However, it must be noted that wavebands that are redundant for one application (e.g., agriculture), may be very valuable in another application (e.g., geology).

It is obvious that there is a need for Whole Spectral Analysis (WSA) as well as Optimal Spectral Analysis (OSA). WSA is of great value under certain conditions such as when: (a) the ability exists to use integrated spectra over a continuum (e.g., integrating spectra over 500 to 600 nm), (b) accurate spectral libraries exist to match class spectra with target spectra from spectral library, (c) spectral signature over an entire spectral range such as 400 to 2500 nm wavelengths are preferred, (d) the Hughes' phenomenon can be overcome by using very large training and accuracy assessment sample sizes, and (e) massive computing power exists to overcome handling very large data volumes. OSA (Table 2) is preferred in situations involving factors such as when: (i) large number of HNBs are redundant (as is often the case for a given application), (ii) overcoming Hughes' phenomenon (e.g., when training samples for classification and accuracy assessment are insufficient in dealing with very large dimensions of hyperspectral data), (iii) specific physiologically meaningful HVIs are required, and (iv) clear efficiency of working with non-redundant bands is meaningful and facilitates rapid applications of data without making significant compromise in classification or modeling accuracies.

“The future of remote sensing is likely to involve regular and routine acquisition of hyperspectral data from which broadbands (e.g., Landsat bands) are simulated. This is a “win win” situation providing data continuity for the past satellites and at the same time providing advanced spectral signatures needed for increased understanding of global vegetation and agriculture”.

It is obvious that there are inadequate hyperspectral libraries at present and there is a clear need to establish hyperspectral libraries of vegetation and agricultural crops that take into consideration a wide array of factors such as, for example, crop types, genotypes, phenology, background influences, and consistency of platform from which the data is acquired.

Spaceborne hyperspectral data acquisition is likely to be a preferred option due to its consistency and global coverage. Issues of cloud cover will be addressed to significant extent through constellations acquiring data throughout the growing period of crops, for example, along with advanced processing schemes.

The future of remote sensing may involve regular and routine acquisition of hyperspectral data from which broadbands (e.g., Landsat bands) are simulated. In such a case, broadbands can be used for data continuity studies of existing systems such as the Landsat or IKONOS or Resourcesat, whereas hyperspectral data and its derivatives (e.g., specific HNBs, HVIs, hyperspectral libraries of species types and crop types) are used for advanced studies of agricultural crop and vegetation classification, monitoring, modeling, and mapping.

REFERENCES

- Atzberger, C. 2013. Advances in Remote Sensing of Agriculture: Context Description, Existing Operational Monitoring Systems and Major Information Needs, *Remote Sensing*, 5(2): 949-981.
- Bajwa and Kulkarni 2011 Hyperspectral data mining, Pp. 93-120 in *Hyperspectral Remote Sensing of Vegetation*, P.S. Thenkabail, et al., Eds., ed: CRC Press- Taylor and Francis group, Boca Raton, London, New York, 781p.
- Banskota, A., Wynne, R., Thomas, V., Serbin, S., Kayastha, N., Gastellu-Etchegorry, J. and Townsend, P. 2013. Investigating the Utility of Wavelet Transforms for Inverting a 3-D Radiative Transfer Model Using Hyperspectral Data to Retrieve Forest LAI, *Remote Sensing*, 5(6): 2639-2659.
- Bian, M., Skidmore, A.K., Schlerf, M., Fei, T., Liu, Y. and Wang, T. 2010. Reflectance spectroscopy of biochemical components as indicators of tea (*Camellia Sinensis*) quality, *Photogrammetric Engineering and Remote Sensing*, 76(12): 1385-1392.
- Blackburn, G.A. 2007. Hyperspectral remote sensing of plant pigments, *Journal of Experimental Botany*, 58(4): 855-867.
- Bolton, D.K. and Friedl, M.A. 2013. Forecasting crop yield using remotely sensed vegetation indices and crop phenology metrics, *Agricultural and Forest Meteorology*, 173(0): 74-84.
- Bruzzone, L., Conese, C., Maselli, F. and Roli, F. 1997. Multi-source classification of complex rural areas by statistical and neural network approaches. , *Photogrammetric Engineering and Remote Sensing*, 65(5): 523-533.
- Burger, J. and Gowen, A. 2011. Data handling in hyperspectral image analysis, *Chemometrics and Intelligent Laboratory Systems*, 108(1): 13-22.

- Clark, M.L. and Roberts, D.A. 2012. Species-Level Differences in Hyperspectral Metrics among Tropical Rainforest Trees as Determined by a Tree-Based Classifier, *Remote Sensing*, 4(6): 1820-1855.
- Congalton, R.G. and Green, K. 1999 Assessing the accuracy of remotely sensed data: principles and practices. in *New York: Lewis*.
- Congalton, R.G. and Green, K. 2008 Assessing the Accuracy of Remotely Sensed Data: Principles and Practices, CRC Press, London, 208 pp.
- Cook, B., Corp, L., Nelson, R., Middleton, E., Morton, D., McCorkel, J., Masek, J., Ranson, K., Ly, V. and Montesano, P. 2013. NASA Goddard's LiDAR, Hyperspectral and Thermal (G-LiHT) Airborne Imager, *Remote Sensing*, 5(8): 4045-4066.
- Delalieux, S., Auwerkerken, A., Verstraeten, W., Somers, B., Valcke, R., Lhermitte, S., Keulemans, J. and Coppin, P. 2009. Hyperspectral Reflectance and Fluorescence Imaging to Detect Scab Induced Stress in Apple Leaves, *Remote Sensing*, 1(4): 858-874.
- Galvão, L.S. 2011 Crop type discrimination using hyperspectral data. Chapter 17. pp. 397-422, in *Hyperspectral Remote Sensing of Vegetation*, P.S. Thenkabail, et al., Eds., ed: CRC Press- Taylor and Francis group, Boca Raton, London, New York, 781 p.
- Gitelson, A.A. 2013. Remote estimation of crop fractional vegetation cover: the use of noise equivalent as an indicator of performance of vegetation indices, *International Journal of Remote Sensing*, 34(17): 6054-6066.
- Haboudane, D., Miller, J.R., Pattey, E., Zarco-Tejada, P.J. and Strachan, I.B. 2004. Hyperspectral vegetation indices and novel algorithms for predicting green LAI of crop canopies: Modeling and validation in the context of precision agriculture, *Remote Sensing of Environment*, 90(3): 337-352.
- Hecker, C.A., Smith, T.E.L., Ribeiro da Luz, B. and Wooster, M.J. 2013 Chapter 3: Thermal infrared spectroscopy in the laboratory and field in support of land surface remote sensing. In C. Kuenzer and S. dech (eds.), *Thermal Infrared remote Sensing: Sensors, methods, Applications, Remote Sensing and Digital Image Processing 17*, DOI 10.1007/978-94-007-6639-6_3, @ Springer Science+Business Media Dordrecht 2013.
- Hook, S.J., Johnshon, W.R. and Abrams, M.J. 2013 Chapter 5: NASA's Hyperspectral Thermal Emission Spectrometer (HyTES) In C. Kuenzer and S. dech (eds.), *Thermal Infrared remote Sensing: Sensors, methods, Applications, Remote Sensing and Digital Image Processing 17*, DOI 10.1007/978-94-007-6639-6_3, @ Springer Science+Business Media Dordrecht 2013.
- Mariotto, I., Thenkabail, P.S., Huete, A., Slonecker, E.T. and Platonov, A. 2013. Hyperspectral versus multispectral crop-productivity modeling and type discrimination for the HypIRI mission, *Remote Sensing of Environment*, 139(0): 291-305.
- Marshall, M.T. and Thenkabail, P. 2014. Biomass modeling of four water intensive crops using hyperspectral narrowbands. , *Photogrammetric Engineering and Remote Sensing*, 80(8): 757-772.
- Middleton, E.M., Ungar, S.G., Mandl, D.J., Ong, L., Frye, S.W., Campbell, P.E., Landis, D.R., Young, J.P. and Pollack, N.H. 2013. The Earth Observing One (EO-1) Satellite Mission: Over a Decade in Space *IEEE Selected Topics in Applied Earth Observations and Remote Sensing*. 6 (2): 427-438.
- Miphokasap, P., Honda, K., Vaiphasa, C., Souris, M. and Nagai, M. 2012. Estimating Canopy Nitrogen Concentration in Sugarcane Using Field Imaging Spectroscopy, *Remote Sensing*, 4(6): 1651-1670.
- Mirzaie, M., Darvishzadeh, R., Shakiba, A., Matkan, A.A., Atzberger, C. and Skidmore, A. 2014. Comparative analysis of different uni- and multi-variate methods for estimation of vegetation water content using hyper-spectral measurements, *International Journal of Applied Earth Observation and Geoinformation*, 26(0): 1-11.
- Mundt, J., Streutker, D.R. and Glenn, N.F. 2006. Mapping sagebrush distribution using fusion of hyperspectral and lidar classifications. , *Photogrammetric Engineering and Remote Sensing* 72: 47-54.
- Nielsen, A. 2001. Spectral Mixture Analysis: Linear and Semi-parametric Full and Iterated Partial Unmixing in Multi- and Hyperspectral Image Data, *International Journal of Computer Vision*, 42(1-2): 17-37.
- Ortenberg, F. 2011 Hyperspectral sensor characteristics: Airborne, Spaceborne, Hand-held, and truck mounted: Integration of hyperspectral data with Lidar. Pp. 39-68. in *Hyperspectral Remote Sensing of Vegetation*, Pp. 561-578 in P. S. Thenkabail, J. G. Lyon, and A. Huete, Eds. Boca Raton, London, New York: CRC Press/Taylor and Francis Group, 2011, ch.23, 561-578 pp.
- Plaza, A., Benediktsson, J.A., Boardman, J.W., Brazile, J., Bruzzone, L., Camps-Valls, G., Chanussot, J., Fauvel, M., Gamba, P., Gualtieri, A., Marconcini, M., Tilton, J.C. and Trianni, G. 2009. Recent advances in techniques for hyperspectral image processing, *Remote Sensing of Environment*, 113, Supplement 1(0): S110-S122.
- Poças, I., Cunha, M. and Pereira, L.S. 2012. Dynamics of mountain semi-natural grassland meadows inferred from SPOT-VEGETATION and field spectroradiometer data, *International Journal of Remote Sensing*, 33(14): 4334-4355.
- Pu, R. and Bell, S. 2013. A protocol for improving mapping and assessing of seagrass abundance along the West Central Coast of Florida using Landsat TM and EO-1 ALI/Hyperion images, *ISPRS Journal of Photogrammetry and Remote Sensing*, 83(0): 116-129.
- Qi, J. 2011. Hyperspectral remote sensing in global change studies (P. S. Thenkabail, et. al., editors), CRC Press-Taylor and Francis group, New York, N.Y., 561-578, 781 pp.
- Ribeiro da Luz, B. and Crowley, J.K. 2010. Identification of plant species by using high spatial and spectral resolution thermal infrared (8.0–13.5 μm) imagery, *Remote Sensing of Environment*, 114(2): 404-413.

- Roberts, D.A. 2011 Hyperspectral vegetation indices. Chapter 14. pp. 309-328, in *Hyperspectral Remote Sensing of Vegetation*, P.S. Thenkabail, et al., Eds., ed: CRC Press- Taylor and Francis group, Boca Raton, London, New York. 781, 2011 pp.
- Schlemmer, M., Gitelson, A., Schepers, J., Ferguson, R., Peng, Y., Shanahan, J. and Rundquist, D. 2013. Remote estimation of nitrogen and chlorophyll contents in maize at leaf and canopy levels, *International Journal of Applied Earth Observation and Geoinformation*, 25(0): 47-54.
- Schlerf, M., Rock, G., Lagoux, P., Ronellenfisch, F., Gerhards, M., Hoffmann, L. and Udelhoven, T. 2012. A Hyperspectral Thermal Infrared Imaging Instrument for Natural Resources Applications, *Remote Sensing*, 4(12): 3995-4009.
- Slonecker, E.T., Fisher, G.B., Marr, D.A., Milheim, L.E. and Roig-Silva, C.M. 2013 Advanced and applied remote sensing of environmental conditions: U.S. Geological Survey Fact Sheet 2013-3007, 2 pp., available only at <http://pubs.usgs.gov/fs/2013/3007/>.
- Staenz, K. and Held, A. 2012. Summary of current and future terrestrial civilian hyperspectral spaceborne systems, *Geosciences and Remote sensing Symposium (IGARSS)*. 123-126. ISSN: 2153-6996.
- Swatantran, A., Dubayah, R., Roberts, D., Hofton, M. and Blair, J.B. 2011. Mapping biomass and stress in the Sierra Nevada using lidar and hyperspectral data fusion, *Remote Sensing of Environment*, 115(11): 2917-2930.
- Thenkabail, P.S. 2002. Optimal Hyperspectral Narrowbands for Discriminating Agricultural Crops, *Remote Sensing Reviews*, 20(4): 257-291.
- Thenkabail, P.S., Enclona, E.A., Ashton, M.S., Legg, C. and De Dieu, M.J. 2004. Hyperion, IKONOS, ALI, and ETM+ sensors in the study of African rainforests, *Remote Sensing of Environment*, 90(1): 23-43.
- Thenkabail, P.S., Enclona, E.A., Ashton, M.S. and Van Der Meer, B. 2004. Accuracy assessments of hyperspectral waveband performance for vegetation analysis applications, *Remote Sensing of Environment*, 91(3-4): 354-376.
- Thenkabail, P.S., Lyon, G.J. and Huete, A. 2011 Book Chapter # 28: Hyperspectral Remote Sensing of Vegetation and Agricultural Crops: Current Status and Future Possibilities. In Book entitled: "Remote Sensing of Global Croplands for Food Security" (CRC Press- Taylor and Francis group, Boca Raton, London, New York. Edited by Thenkabail, P.S., Lyon, G.J., and Huete, A. 663-668 pp.
- Thenkabail, P.S., Lyon, G.J. and Huete, A. 2011 *Book entitled: "Hyperspectral Remote Sensing of Vegetation". CRC Press-Taylor and Francis group, Boca Raton, London, New York. Pp. 781 (80+ pages in color). Reviews of this book: <http://www.crcpress.com/product/isbn/9781439845370>.*
- Thenkabail, P.S., Mariotto, I., Gumma, M.K., Middleton, E.M., Landis, a.D.R. and Huemmrich, F.K. 2013. Selection of hyperspectral narrowbands (HNBS) and composition of hyperspectral twoband vegetation indices (HVIs) for biophysical characterization and discrimination of crop types using field reflectance and Hyperion/EO-1 data, *IEEE Journal of Selected Topics in Applied Earth Observations and Remote Sensing*, 6(2): 427-438.
- Thenkabail, P.S., Smith, R.B. and De-Pauw, E. 2002. Evaluation of Narrowband and Broadband Vegetation Indices for Determining Optimal Hyperspectral Wavebands for Agricultural Crop Characterization, *Photogrammetric Engineering and Remote Sensing*, 68(6): 607-621.
- Thenkabail, P.S., Smith, R.B. and De Pauw, E. 2000. Hyperspectral Vegetation Indices and Their Relationships with Agricultural Crop Characteristics, *Remote Sensing of Environment*, 71(2): 158-182.
- Thorp, K.R., French, A.N. and Rango, A. 2013. Effect of image spatial and spectral characteristics on mapping semi-arid rangeland vegetation using multiple endmember spectral mixture analysis (MESMA), *Remote Sensing of Environment*, 132(0): 120-130.
- Udelhoven, T., Delfosse, P., Bossung, C., Ronellenfisch, F., Mayer, F., Schlerf, M., Machwitz, M. and Hoffmann, L. 2013. Retrieving the Bioenergy Potential from Maize Crops Using Hyperspectral Remote Sensing, *Remote Sensing*, 5(1): 254-273.
- Verrelst, J., Romijn, E. and Kooistra, L. 2012. Mapping Vegetation Density in a Heterogeneous River Floodplain Ecosystem Using Pointable CHRIS/PROBA Data, *Remote Sensing*, 4(9): 2866-2889.
- Zhang, B., Wang, X., Liu, J., Zheng, L. and Tong, Q. 2000. Hyperspectral Image Processing and Analysis System (HIPAS) and its application, *Photogrammetric Engineering and Remote Sensing*, 66(5): 605-619.
- Zhang, C., Kovacs, J., Wachowiak, M. and Flores-Verdugo, F. 2013. Relationship between Hyperspectral Measurements and Mangrove Leaf Nitrogen Concentrations, *Remote Sensing*, 5(2): 891-908.

AUTHORS

Prasad S. Thenkabail, Western Geographic Science Center, U. S. Geological Survey, USA

Murali Krishna Gumma, International Crops Research Institute for the Semi-Arid Tropics (ICRISAT)

Pardhasaradhi Teluguntla, Western Geographic Science Center, U. S. Geological Survey, and the Bay Area Environmental Research Institute (BAERI), California, USA

Irshad A. Mohammed, International Crops Research Institute for the Semi-Arid Tropics (ICRISAT)

Research Advances in Hyperspectral Remote Sensing

Prasad S. Thenkabail

Hyperspectral data provides substantially increased understanding of plant biophysical and biochemical properties relative to multispectral broadband data. Accuracies in classifying, modeling, mapping, and monitoring are substantially higher when specific hyperspectral narrowbands (HNBs) and hyperspectral vegetation indices (HVIs) are used as opposed to multispectral broadbands. Even though this is now a well-established fact, there is still significant knowledge gap in our understanding of the importance hyperspectral data in study of agricultural crops and vegetation (Thenkabail et al., 2011). Indeed, opportunities exist for making significant knowledge advances in several areas of hyperspectral study of vegetation and agricultural crops such as in: 1. Establishing specific HNBs and HVIs to quantify biophysical and biochemical properties, 2. Overcoming Hughes' phenomenon and data redundancy, 3. Building hyperspectral libraries of crops and vegetation, and 4. Developing advanced automated methods of hyperspectral data analysis. Also, increasing amounts of hyperspectral data (e.g., entire archive of ~64,000 images of EO-1 Hyperion available from USGS Earthexplorer (<http://earthexplorer.usgs.gov/>); see highlight article in this issue for details) are becoming available, globally, for researchers around the world to conduct specific studies on specific issues in different croplands and vegetation of the world. Given this fact, the need for focused research to better understand, model, and map specific vegetation and agricultural crop characteristics utilizing hyperspectral data is of great importance. In this context, PE&RS initiated this special issue on the topic. The special issue covers some of these advances through seven distinct peer-reviewed articles. Highlights of these seven peer-reviewed articles along with their key knowledge advancement are summarized below.

1.0 Automated Hypercor Algorithm to Process Large Volumes of Hyperspectral Data and Identify Important Bands to Model Biophysical and Biochemical Quantities and a Novel Concept of Multi-Correlation Matrices Strategy (MCMS) to Select and use Hyperspectral Narrowbands (HNBs) in Hyperspectral Vegetation Indices (HVIs)

Aasen et al. developed automated algorithms to process large volumes of hyperspectral data in order to determine which hyperspectral narrowbands (HNBs) and/or hyperspectral vegetation indices (HVIs) hold the best information. They developed an impressive algorithm called HyperCor to process large volumes of hyperspectral data and discern their information pathways. HyperCor takes hundreds or thousands of HNBs, computes their two-band or multi-band HVIs, correlates with biophysical and biochemical quantities of vegetation or agricultural crops, and shows us the windows or regions in electromagnetic spectrum providing high and low information content. This is exactly the type of tool that we

need to make best and most efficient use of hyperspectral data in applications such as the vegetation, and the agricultural crops. Their study on rice crop was conducted with 5 years of solid data (3 years for model development and 2 years for validation). In selecting best HNBs, it must be noted that the HNBs which are most prominent for one biophysical quantity may not be the most prominent for another biophysical quantity. At times, it may not even be most prominent for the same biophysical quantity in another date. This phenomenon happens as a result of having narrowbands adjacent to one another providing near similar information (e.g., 680 nm and 690 nm are likely to have equally good correlation with biomass). This will require us to select the most prominent narrowband in each spectral range (e.g., a band centered at 680 nm, with 10 nm bandwidth, could be most frequently occurring narrowband in modeling biophysical and biochemical properties of vegetation and agricultural crop in 600 to 700 nm band range). Overall, they clearly established that automated algorithms like HyperCor are extremely valuable in analyzing biophysical and biochemical variables of massive volumes of hyperspectral data of agricultural crops and vegetation. They also introduced a novel concept of multi-correlation matrices strategy (MCMS) to select and use HNBs in HVIs. The idea here is to source the importance of HNBs based on their significant occurrence in different correlation matrices (CMs). They showed that MCMS provided significantly improved accuracies in studying rice biomass. MCMS is an interesting concept, but requires further development. Aasen et al. developed their models using various approaches: pooled data of various growth stages, individual growth stages, linear models, and non-linear models. It must be noted that robust models of biophysical and biochemical properties of specific crops need to be developed, ideally, taking data of across sites and across growing stages. Such models are also often nonlinear in nature as a result of saturation in reflectivity in full canopy cover scenario. Also, such models need to be developed for individual crops rather than grouping multiple crop types in models to achieve best results that are specific and targeted.

2.0 Automatic Labeling of Classes through Spectral Matching Techniques (SMTs) by using Ideal Spectra from Spectral Library

It is well known that hyperspectral data is not panacea for addressing complex issues of cropland and vegetation classification, modeling, and characterization. This is because, even though hyperspectral data provides a quantum leap in information, discerning that information is not an easy task given the complexities of processing massively large data volumes, establishing redundant bands, and implementing methods and techniques that accurately and rapidly establish information from data. In this regard the work of Parshakov

et al. is invaluable. They have implemented an innovative spectral matching technique (SMT; also see Thenkabail et al., 2007 for concept of SMTs) approach that automatically determines and labels crop types by matching the class spectral signatures with the ideal or reference spectral libraries developed using hyperspectral Hyperion data. The Z-score distance SMT that they use accounts for the variation of pixel spectra by measuring the distance between the class spectra and the reference spectra in units of standard deviation. They used this SMT method to identify and label 11 agricultural crops classified using Landsat TM data. Their study established that the accuracies of their automated SMT provided: A. 6 to 11 percent greater accuracies relative to ISODATA classification followed by manual identification of classes, and B. 12 percent greater than the spectral angle mapper (SAM) followed by manual identification of classes. However, the accuracies were 2 to 12% lower than the Maximum Likelihood Classification followed by manual class identification. Their method can be used to automatically identify and label classes classified using multispectral or hyperspectral data. The automated SMT by Parshakov et al. is novel and clearly demonstrates pathway to identify and label crop types and other land use classes automatically saving time and removing user bias. However, there will be complexities of applying automated SMTs over large and complex areas. Nevertheless, by building adequate and accurate ideal or reference spectral libraries of agricultural crops, vegetation categories, and other land use classes as well as by further development of automated SMTs for specific regions of the world, automated class labeling proposed and demonstrated by Parshakov et al. will become accurate, unbiased, rapid, and widely implementable.

3.0 Methods for Data Dimensionality Reduction and Overcoming Hughes' Phenomenon

The study by Nadiminti et al. address the important issue of high dimensionality of hyperspectral data, ways and approaches to overcome them, and the benefit of doing so to overcome Hughes Phenomenon (Note: Hughes phenomenon means that when the dimensionality of data increases, the training sample number should also increase in order to maintain precision of classification, alternatively we need to increase the number of training samples which can be often resource prohibitive. Thereby, in order to process hyperspectral data effectively, it is necessarily to reduce the dimensionality of hyperspectral data or increase the sample number of training data used in classification. Including highly correlated bands (e.g., R-square >0.9) in analysis either makes no difference to classification accuracies or, many a times, actually leads to decrease in classification accuracies. This is because highly correlated bands provide same, duplicate, information whereas the training samples remain the same in spite of increase in number of bands. Nadiminti et al. used hyperspectral Hyperion images of three seasons (Monsoon, winter, and summer) over tropical forests to classify and separate three species: Teak, Bamboo, and mixed forests. Data dimensionality reduction was explored using Kernel Principal Component Analysis (k-PCA), Independent Component Analysis (ICA), and Principal Component Analysis (PCA). Their results re-enforced the recent findings elsewhere (Thenkabail et al., 2013) that 4 to 8 % hyperspectral narrowbands (HNBs) provide optimal results, leaving the rest of the bands redundant. In kPCA, for example, 10 kernel principal components or HNBs, selected based on eigenvectors (factor loadings), explained 99% variability in data when 179 Hyperion HNBs were used in analysis. Thereby, the study establishes the fact that, often, HNBs that

adjoin one another are redundant for a given application. Thereby, identifying redundant bands help overcome Hughes' Phenomenon.

4.0 Significantly Improved Vegetation Classification Accuracies by Combining Hyperspectral Data with LiDAR

Hyperspectral data is in itself a great advancement over broadband multispectral data. This is now an established fact (Thenkabail et al., 2011). Nevertheless, there is considerable scope for improvement in our understanding of agricultural crops and vegetation communities by combining multiple sources of remote sensing data. This aspect is well illustrated by Zhang et al. in their paper on studying wetland vegetation communities of Florida everglades by combining hyperspectral data with Light Detection and Ranging (LiDAR) data. They studied 13 common everglades vegetation communities using 224 band hyperspectral Airborne Visible/Infrared Imaging Spectrometer (AVIRIS) data acquired at 12 m spatial resolution and a Leica ALS-50 LiDAR system collecting small footprint multiple returns, and intensity at 1060 nm wavelength with average point density for the study area of 1.18 pts/m². They showed by fusing the hyperspectral and LiDAR data and using the 3 machine learning algorithms [Random Forest (RF), Support Vector Machine (SVM), and *k*-Nearest Neighbor (*k*-NN)] it is possible to increase the overall accuracy by as much as 10% (from 76% overall accuracy using Hyperspectral data alone to 86% when both Hyperspectral and LiDAR are used) in classifying 13 everglade wetland vegetation communities.

5.0 Advances in Soil Moisture Retrieval from Irrigated-, Rainfed-, and Fallow Agricultural Farmlands by Combining Hyperspectral Data with Thermal and Radar Data

Sanchez et al. combined hyperspectral data with thermal and radar data to retrieve soil moisture from agricultural fields. They used data from Compact Airborne Spectrographic Imager (CASI 550) sensor and Thermal Airborne Spectrographic Imager (TASI 600) and combined with Airborne L-band (ARIEL-2) to retrieve soil moisture from irrigated-, rainfed-, and fallow- farmlands that include cereals, sunflower, vineyards, and fallow-farmlands. They showed that hyperspectral bands and indices (HNBs and HVIs) had significantly better correlation with observed soil moisture when integrated with the land surface temperature (LST) and brightness temperature (BT) rather than when they were used alone. They specifically recommend indices derived using hyperspectral wavebands in the red-edge and near infrared rather than visible. Even through microwave L-band data is widely used for soil moisture retrieval, using that data along with hyperspectral data has significant advantages.

6.0 Significantly Increased Classification Accuracies of Pine Forests using Hyperspectral Narrowbands as Opposed to Multispectral Broadbands

Awad et al. clearly establish that classification accuracies can be substantially increased using hyperspectral narrowband data as opposed to multispectral broadband data. They used CHRIS PROBA hyperspectral data to classify Stone Pine forests and compare the results with Landsat ETM+ classified results. Using the 63 band spaceborne CHRIS PROBA hyperspectral data they were able to establish an increased accuracy of as much as about 30%. The producer's, User's, and overall accuracies in classifying stone pine forests using CHRIS PROBA were 90% or higher whereas using 6 non-thermal Landsat ETM+ these accuracies were around 60%.

7.0 Significantly Improved Biomass Modelling of Four Leading World Crops using Hyperspectral Narrowbands (HNBs) and hyperspectral Vegetation Indices (HVIs)

Hundreds of HNBs and HVIs were used model above-ground biomass of 4 leading world crops (rice, wheat, corn, alfalfa) based on 2 years of detailed data acquired for these crops in the irrigated agricultural fields of California by Marshall and Thenkabail. The best biomass models explained greater than 80% variability using highly selective sequential search methods (SSM) involving two-band HVIs or multi-band HVIs involving one to 3 HNBs. The key is also to select specific narrowbands (~10 nm or less) from two or three distinct portion of the spectrum: (a) green and near-infrared, (b) blue and NIR, (c) near-infrared (NIR) and short-wave infrared (SWIR), or (d) green, NIR, and SWIR. These specific HNBs may change for crop to crop and even within crop. But, what needs to be noted is that there are some very selective HNBs and HVIs derived off them (see the Table 2 and 3 in the highlight article of this issue) which consistently perform highly across different crops and their varying characteristics. The HNBs and HVIs vary because selecting one HNB versus another often makes only a slight difference (e.g., 680 nm or 690 nm are highly correlated and perform about the same; similarly 855 nm or 910 nm are highly correlated and perform similarly; a point also noted in other reported studies). But, in modelling a specific crop an HVI involving 855 nm and 680 nm (HVI855680) may perform marginally better than an HVI involving 910 nm and 690 nm (HVI910690). This performance may, at times differ for another crop. This does not mean that we need to use both the indices. It will suffice to use a single index (e.g., HVI855680) to model both crops because the two HVIs are equally good (e.g., one index may have an R-square of 0.85 with biomass and another 0.87; in which case we will select the one with 0.87 and ignore the one with 0.85). The study by Marshall and Thenkabail, re-affirms the fact that there are redundant bands as well as there are specific HNBs that are of highest importance to model specific biophysical and biochemical characteristics of crops or vegetation. These HNBs and HVIs perform significantly better than any known broadband derived indices. Readers should refer to various Tables and figures of the paper by Marshall and Thenkabail for better understanding. Further, greater, comprehensive understanding can be acquired by going through Table 2, 3, and 4 as well as Figure 4a and 4b of the highlight article in this special issue.

Hyperspectral remote sensing (or Imaging Spectroscopy) is fast moving from an era of research into an era of applications. Many spaceborne hyperspectral sensors (e.g., HypSPiRI, UAV based platforms, interest from private entities; see Thenkabail et al., 2011) are planned in near future. This special issue adds to maturing knowledge of hyperspectral remote sensing in general, and hyperspectral remote sensing of vegetation and agricultural crops in particular.

Credit to this special issue on “**Hyperspectral Remote Sensing of Vegetation and Agricultural Crops**” goes to several people. I would like to thank the authors for their outstanding work. Each paper was reviewed by at least 3 reviewers. Good reviewers are few but pivotal for success of any quality journal. I am thankful to many good reviewers who helped improve the quality of each paper. I am grateful for the advice, support, and guidance of Dr. Russell Congalton, Editor in Chief of PE&RS. Ms. Jeanie G. Congalton, PE&RS manuscript coordinator, was always there with her insights. Finally, I would like to thank the U. S. Geological Survey (USGS), especially USGS Western Geographic Science Center (WGSC) and its leadership, for all the opportunities and encouragement that I have received over the years.

7.0 References:

- Middleton, E.M.; Ungar, S.G.; Mandl, D.J.; Ong, L.; Frye, S.W.; Campbell, P.E.; Landis, D.R.; Young, J.P.; Pollack, N.H., 2013. “The Earth Observing One (EO-1) Satellite Mission: Over a Decade in Space,” *Selected Topics in Applied Earth Observations and Remote Sensing, IEEE Journal of*, vol.6, no.2, pp.243,256, April 2013. doi: 10.1109/JSTARS.2013.2249496
- Thenkabail, P.S., Lyon, G.J., and Huete, A. 2011. Book entitled: “Hyperspectral Remote Sensing of Vegetation”. CRC Press- Taylor and Francis group, Boca Raton, London, New York. Pp. 781 (80+ pages in color).
Reviews of this book: <http://www.crcpress.com/product/isbn/9781439845370>
- Thenkabail, P.S., Mariotto, I., Gumma, M.K., Middleton, E.M., Landis, and D.R., Huemmrich, F.K., 2013. Selection of hyperspectral narrowbands (HNBs) and composition of hyperspectral twoband vegetation indices (HVIs) for biophysical characterization and discrimination of crop types using field reflectance and Hyperion/EO-1 data. *IEEE JOURNAL OF SELECTED TOPICS IN APPLIED EARTH OBSERVATIONS AND REMOTE SENSING*, Pp. 427-439, VOL. 6, NO. 2, APRIL 2013. doi: 10.1109/JSTARS.2013.2252601.
- Thenkabail, P.S., GangadharaRao, P., Biggs, T., Krishna, M., and Turrall, H., 2007. Spectral Matching Techniques to Determine Historical Land use/Land cover (LULC) and Irrigated Areas using Time-series AVHRR Pathfinder Datasets in the Krishna River Basin, India. *Photogrammetric Engineering and Remote Sensing*. 73(9): 1029-1040.

Special Issue Editor

Dr. Prasad S. Thenkabail
Research Geographer
U. S. Geological Survey

Email: pthenkabail@usgs.gov; Thenkabail@gmail.com